Nonlinear Dyn (2011) 64: 177–195
DOI 10.1007/s11071-010-9856-6

ORIGINAL PAPER

Response regimes in forced system with non-linear energy sink: quasi-periodic and random forcing

Y. Starosvetsky · O.V. Gendelman

Received: 15 June 2010 / Accepted: 20 September 2010 / Published online: 14 October 2010

Abstract The system under investigation comprises a linear oscillator coupled to a non-linear energy sink (NES) under quasi-periodic forcing in the regime of 1:1:1 resonance. Interaction of the quasi-periodic excitation with the strongly modulated response (SMR) regime is studied in detail both analytically and numerically. Theoretical study developed in the paper allows establishing the threshold value for the amplitude of modulation beyond which SMR regime is excited. This phenomenon is of great practical use since applying the quasi-periodic excitation beyond the threshold results in elimination of possible undesired regimes causing high-amplitude oscillations of the main structure. Bifurcations of the SMR caused by quasi-periodic excitation were analyzed with the help of semi-analytical procedure based on two-dimensional maps. Numerical evidences for exciting the strongly modulated bursts in the response by a random, quasi-periodic narrow-band excitation are also provided. Fairly good correspondence was observed between analytical model and numerical simulations.

Y. Starosvetsky
Department of Mechanical Science and Engineering,
University of Illinois at Urbana-Champaign,
Urbana, IL 61820, USA

O.V. Gendelman (✉)
Faculty of Mechanical Engineering, Technion—Israel
Institute of Technology, Technion City, Haifa 32000, Israel
e-mail: ovgend@tx.technion.ac.il

Keywords Targeted energy transfer · Non-linear energy sink · Vibration absorption · Quasi-periodic forcing · Random forcing

1 Introduction

Targeted energy transfer (TET) from the initially excited linear substructure to a strongly non-linear lightweight mass attachment has been extensively studied for the last decade [1–6]. These studies gave rise to a new concept of non-linear energy sink (NES). Recently the ideas of targeted energy transfer found successful implementations not only in vibration attenuation of the unwanted mechanical vibrations but also in the field of acoustics [7] where the aforementioned methodology is used for a passive sound control. In contrast to the targeted energy transfer we would like also to note that addition of the light mass attachment may also assist in vibration isolation designs where the idea of strong (non-linearizable) non-linearity is studied in relationship to isolation of the non-linear attachment from the harmonically excited linear substructure [8]. The dynamics of slightly different non-linear system comprising light mass non-linear element with geometrical non-linearity attached to the shaker which was driven harmonically has been studied in [9].

It was also demonstrated [2–4] that the possibility of the energy pumping phenomenon in non-conservative systems can be understood and explained by studying the energy dependence of the non-linear,

un-damped free periodic solutions (non-linear normal modes (NNM)) of the corresponding conservative system which are obtained when all damping forces are eliminated. Recent studies [10] based on the approach of invariant manifolds [11, 12] has introduced an asymptotic procedure suitable for the explicit inclusion of damping within the framework of non-linear normal modes (NNMs).

Simple periodic responses (i.e. the responses with almost constant amplitude) of the primary linear oscillator subject to a trivial harmonic excitation with NES attached were studied previously in [13]. In recent studies it was demonstrated [14, 15] that in the close vicinity of the fundamental (1:1) resonance surface the system comprising linear oscillator subject to harmonic excitation with NES attached may exhibit weakly modulated motions (quasi-periodic) rather than simple periodic-response regimes. In papers [16, 17] it was established that the combination of essential non-linearity and strong mass asymmetry brings about a possibility of response regimes qualitatively different from simple periodic and weakly modulated responses—existing in the vicinities of fundamental 1:1 resonance. Obviously, these extremely unusual response regimes characterized by deep amplitude of modulation cannot be described with the help of local analysis of the slow-flow equations. The most appropriate way of treating these motions is from the viewpoint of relaxation oscillations, i.e. switches between slow motions at stable critical manifolds of the system and fast jumps between them. It is possible to distinguish the "slow" and the "fast" time scales due to a small parameter related to the mass ratio. These response regimes were referred to as a strongly modulated response (SMR). In paper [16] however it was demonstrated that such a response maybe in fact multi-locked (due to phase locking) or even chaotic.

In paper [17] it was demonstrated numerically that the SMR exists in the vicinity of the exact 1:1 resonance and sometimes is very favorable from viewpoint of vibration absorption and mitigation (better than tuned linear absorber). A semi-analytical approach for analysis of the SMR was developed in [18], allowing the systematic study of the stability of the SMR and its global bifurcations. Series of additional studies based on this approach were carried out in [19, 20]. These studies have extended the system under consideration to three degrees of freedom under different conditions of internal resonances and forcing. The effect of the mass of the NES on the global bifurcations of SMR has been investigated both analytically and numerically in [21].

One of the major drawbacks of using NES as a vibration absorber reported in several recent works is an existence of simple periodic-response regimes of rather high amplitudes exhibited by a linear substructure. One of the proposed solutions to overcome that was an inclusion of non-linear damping in the system under investigation [22].

We suggest another tool for coping with the unwanted periodic-response regimes. All recent studies dealing with the dynamics of the harmonically forced 2DOF and 3DOF systems comprising the excited linear substructure and the NES attached dealt with simple harmonic external forcing. In the present paper we study the dynamics of the system comprising linear oscillator given to a quasi-periodic excitation (two harmonic forces with closely spaced frequencies) and the NES attached. As it is demonstrated in the paper, quasi-periodic excitation may be of preference due to its ability to eliminate the undesired periodic-response regimes and to facilitate excitation of the SMR (favorable in a sense of vibration mitigation).

The second section of the paper provides theoretical study of various types of responses existing in the system under investigation. This study allows establishing the threshold value for the amplitude of modulation beyond which SMR regime is excited. This phenomenon is of great practical use since applying the quasi-periodic excitation beyond the threshold results in elimination of possible undesired regimes causing high-amplitude oscillations of the main structure. Certain interesting bifurcations as period doubling of SMR caused by quasi-periodic excitation are revealed. Semi-analytical procedure based on two-dimensional maps is developed for studying these bifurcations. All the theoretical findings of Sect. 2 are verified numerically in Sect. 3. Fairly good agreement between the theoretical and numerical models is observed. System response to the random, narrow-band excitation is also addressed in Sect. 3. It is demonstrated that weakly modulated, random force may cause the effect similar to that of a deterministic, weakly modulated force-elimination of the unwanted response regimes.

2 Description of the model and analytical treatment

Following previous studies [15–21], we consider the linear oscillator subject to a two term, harmonic excitation and attached to a non-linear energy sink with small relative mass, essentially non-linear (pure cubic) spring and linear damping. The two exciting harmonic terms are assumed to have closely spaced frequencies and are situated in the vicinity of the main frequency of linear oscillator. The system under investigation is described by the following non-dimensionalized equations:

$$\begin{aligned}&\ddot{y}_1 + (1+\varepsilon\sigma_1)y_1 + \varepsilon\lambda(\dot{y}_1 - \dot{y}_2) + \frac{4}{3}\varepsilon(y_1 - y_2)^3 \\ &\quad = \varepsilon\big(A_1\cos(t) + A_2\cos\big((1+\varepsilon\sigma_2)t\big)\big), \qquad (1)\\ &\varepsilon\ddot{y}_2 + \varepsilon\lambda(\dot{y}_2 - \dot{y}_1) + \frac{4}{3}\varepsilon(y_2 - y_1)^3 = 0,\end{aligned}$$

where y_1 and y_2 are the displacements of the linear oscillator and the attachment respectively, $\varepsilon\lambda$ is the damping coefficient, $\varepsilon A_1, \varepsilon A_2$ are the amplitudes of external forces and σ_1, σ_2 are the frequencies mismatches parameters. $\varepsilon \ll 1$ is a small parameter which establishes the order of magnitude for coupling, damping, amplitude of the external force, detuning and relative mass of the attachment.

Coefficients: $A_1, A_2, \lambda, \sigma_1, \sigma_2$ are adopted to be of order unity. Rigidity of the non-linear spring is adopted to be equal to $\frac{4}{3}\varepsilon$ and linear frequency of the primary oscillator-close to unity. The latter adoption does not affect the generality of a treatment below, since it may be changed independently by proper rescaling of time and the dependent variables.

Several changes of variables are applied to (1) as follows:

$$v = y_1 + \varepsilon y_2, \qquad w = y_1 - y_2. \qquad (2)$$

We are interested in studying the responses of (1) in the vicinity of (1:1:1 resonance). Therefore it is convenient to introduce another change of variables in the following complex form (Manevitch (1999) [22]).

$$\begin{aligned}&\varphi_1(t)\exp(it) = \dot{v} + iv,\\ &\varphi_2(t)\exp(it) = \dot{w} + iw.\end{aligned} \qquad (3)$$

Assuming that $\varphi_1(t)$, $\varphi_2(t)$ are slowly varying comparing to the frequency of excitation one can derive slow-flow system corresponding to (1) under condition of (1:1) resonance. To this extent introducing (2), (3) into (1) and performing averaging over the fast frequency $\Omega = 1$, one obtains:

$$\begin{aligned}&\dot{\varphi}_1 + \frac{i\varepsilon}{2(1+\varepsilon)}(\varphi_1 - \varphi_2) - \frac{i\varepsilon\sigma(\varphi_1 + \varepsilon\varphi_2)}{2(1+\varepsilon)}\\ &\quad = \frac{\varepsilon(A_1 + A_2\exp(i\varepsilon\sigma_2 t))}{2},\\ &\dot{\varphi}_2 + \lambda(1+\varepsilon)\frac{\varphi_2}{2} + \frac{i}{2(1+\varepsilon)}(\varphi_2 - \varphi_1) \qquad (4)\\ &\quad - \frac{i\varepsilon\sigma(\varphi_1 + \varepsilon\varphi_2)}{2(1+\varepsilon)} - \frac{i(1+\varepsilon)}{2}|\varphi_2|^2\varphi_2\\ &\quad = \frac{\varepsilon(A_1 + A_2\exp(i\varepsilon\sigma_2 t))}{2}.\end{aligned}$$

2.1 Analytical study for the case of single exciting harmonic force ($A_2 = 0$)

For the sake of completeness, we briefly repeat the analysis previously reported in [18] and main results for the case of a single forcing term (i.e. $A_2 = 0$). The following slow-flow system is considered:

$$\begin{aligned}&\dot{\varphi}_1 + \frac{i\varepsilon}{2(1+\varepsilon)}(\varphi_1 - \varphi_2) - \frac{i\varepsilon\sigma(\varphi_1 + \varepsilon\varphi_2)}{2(1+\varepsilon)} = \frac{\varepsilon A_1}{2},\\ &\dot{\varphi}_2 + \lambda(1+\varepsilon)\frac{\varphi_2}{2} + \frac{i}{2(1+\varepsilon)}(\varphi_2 - \varphi_1) \qquad (5)\\ &\quad - \frac{i\varepsilon\sigma(\varphi_1 + \varepsilon\varphi_2)}{2(1+\varepsilon)} - \frac{i(1+\varepsilon)}{2}|\varphi_2|^2\varphi_2 = \frac{\varepsilon A_1}{2}.\end{aligned}$$

Fixed points of (5) correspond to periodic responses of the system described by (1). The investigation of these fixed points and their stability is beyond the scope of this paper—it can be performed by standard methods and will be published elsewhere. System (4) has a somewhat special form-the time derivative in the first equation is proportional to the small parameter and thus the time evolution of variable φ_1 can be considered as slow compared to φ_2. This peculiarity means that the dynamics of System (4) in four-dimensional real state space may be presented in terms of two "fast" and two "slow" real variables, thus giving a chance of tractable global description.

By simple manipulations, System (5) may be reduced to a single second-order ODE:

$$\frac{d^2\varphi_2}{dt^2} + \frac{d}{dt}\left[\alpha\varphi_2 - \frac{i(1+\varepsilon)}{2}|\varphi_2|^2\varphi_2\right.$$

$$+\frac{i\varepsilon}{2(1+\varepsilon)}(1-\sigma)\varphi_2\Bigg]+\frac{i\varepsilon}{2(1+\varepsilon)}(1-\sigma)$$
$$\times\left[\alpha\varphi_2-\frac{i(1+\varepsilon)}{2}|\varphi_2|^2\varphi_2-\frac{\varepsilon A_1}{2}\right]$$
$$-\frac{i\varepsilon\beta}{2(1+\varepsilon)}[1+\varepsilon\sigma]\varphi_2=\frac{\varepsilon A_1\beta}{2}, \tag{6}$$

where

$$\alpha=\frac{\lambda(1+\varepsilon)^2+i-i\varepsilon^2\sigma}{2(1+\varepsilon)},$$
$$\beta=\frac{i}{2(1+\varepsilon)}(1+\varepsilon\sigma).$$

Multiple scale expansion is introduced as:

$$\varphi_2=\varphi_2(\tau_0,\tau_1,\ldots);$$
$$\frac{d}{dt}=\frac{\partial}{\partial\tau_0}+\varepsilon\frac{\partial}{\partial\tau_1}+\cdots, \tag{7}$$
$$\tau_k=\varepsilon^k t,\quad k=0,1,\ldots.$$

Substituting (7) into (6) and equating the like powers of ε one obtains equations for zero and the first order approximations:

$$\varepsilon^0:\quad \frac{\partial^2\varphi_2}{\partial\tau_0^2}+\frac{\partial}{\partial\tau_0}\left[\frac{\lambda\varphi_2}{2}+\frac{i\varphi_2}{2}-\frac{i}{2}|\varphi_2|^2\varphi_2\right]=0,$$
$$\varepsilon^1:\quad 2\frac{\partial^2\varphi_2}{\partial\tau_0\partial\tau_1}+\frac{\partial}{\partial\tau_1}\left[\frac{\lambda\varphi_2}{2}+\frac{i\varphi_2}{2}-\frac{i}{2}|\varphi_2|^2\varphi_2\right]$$
$$+\frac{\partial}{\partial\tau_0}\left[\frac{\lambda\varphi_2}{2}+\frac{i(1-\sigma)\varphi_2}{2}-\frac{i}{2}|\varphi_2|^2\varphi_2\right] \tag{8}$$
$$+\frac{1-\sigma}{4}|\varphi_2|^2\varphi_2+\left[\frac{\sigma}{4}+\frac{i\lambda(1-\sigma)}{4}\right]\varphi_2$$
$$-\frac{iA_1}{4}=0.$$

The first equation of (7) describes "fast" evolution of the averaged system. It can be trivially integrated:

$$\frac{\partial}{\partial\tau_0}\varphi_2+\left(\frac{i}{2}\varphi_2+\frac{\lambda}{2}\varphi_2-\frac{i}{2}|\varphi_2|^2\varphi_2\right)=C(\tau_1,\ldots), \tag{9}$$

where C is arbitrary function of higher-order time scales. Approximations of higher orders are not used in current analysis. Then for the sake of brevity only dependence on time scales τ_0 and τ_1 will be denoted explicitly below. Fixed points $\Phi(\tau_1)$ of (8) depend only on time scale τ_1 and obey algebraic equation:

$$\frac{i}{2}\Phi+\frac{\lambda}{2}\Phi-\frac{i}{2}|\Phi|^2\Phi=C(\tau_1). \tag{10}$$

Equation (9) is easily solved by taking $\Phi(\tau_1)=N(\tau_1)\exp(i\theta(\tau_1))$ and performing trivial calculations:

$$\lambda^2N^4+\left(N^2-N^4\right)^2=4\left|C(\tau_1)\right|^2N^2$$

or, equivalently,

$$\lambda^2Z(\tau_1)+Z(\tau_1)\left(1-Z(\tau_1)\right)^2=4\left|C(\tau_1)\right|^2,$$
$$Z(\tau_1)=\left(N(\tau_1)\right)^2. \tag{11}$$

The expression for argument of the fixed point may be written as

$$\theta(\tau_1)=\arg C(\tau_1)-\tan^{-1}\frac{1-Z(\tau_1)}{\lambda}, \tag{12}$$

where $Z(\tau_1)$ is solution of (11).

Number of solutions of (11) depends on $|C(\tau_1)|$ and λ. Function in the left-hand side can be monotonous or can have maximum and minimum. In the former case the change of $|C(\tau_1)|$ has no effect on the number of solutions (11) will have one positive solution. In the latter case the change of $|C(\tau_1)|$ will bring about a pair of saddle-node bifurcations. In order to distinguish between different cases we should check whether the derivative of the left-hand side of (11) has roots:

$$1+\lambda^2-4Z+3Z^2=0\quad\text{or}$$
$$Z_{1,2}=\frac{2\mp\sqrt{1-3\lambda^2}}{3}. \tag{13}$$

Therefore two roots and pair of saddle-node bifurcations exist for $\lambda<1/\sqrt{3}$ and do not exist otherwise. At critical value $\lambda=1/\sqrt{3}$ two saddle-node bifurcation points coalesce, thus forming a typical structure of a cusp catastrophe.

It is easy to see from (8) if only one solution of (11) exists, it is stable with respect to time scale τ_0. If there are three solutions, two of them are stable (nodes) and one is unstable (saddle). Therefore at time scale τ_0 the phase point will be attracted to one of the nodes. In fact, (9) defines slow invariant manifold (SIM) of the problem. In the case $\lambda<1/\sqrt{3}$ the fold lines $N_{1,2}$:

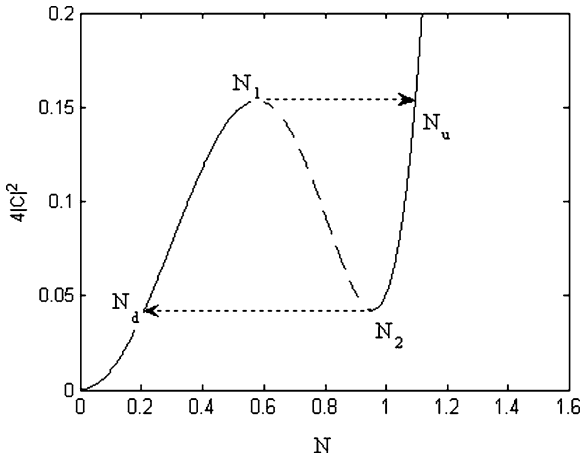

Fig. 1 Projection of the slow invariant manifold of the system in accordance with (10), $\lambda = 0.2$. The unstable branch is denoted by *dashed line*. *Arrows* denote hypothetic "jumps" in the regime of the relaxation oscillations. N_1 and N_2 denote the fold lines, N_u and N_d the final points of the "jumps"

$N(\tau_1) = Z_{1,2}^{1/2}, \theta(\tau_1) \in (0, 2\pi)$ divide stable and unstable branches of the SIM. Figure 1 demonstrates projection of the two-dimensional SIM on the plane (N, C). The fold lines correspond to the points of maximum and minimum.

It is well known [17–19] that such structure of the SIM may give rise to relaxation-type oscillations of the system-the hypothetic "jumps" between the stable branches are denoted by arrows at Fig. 1. N_u and N_d denote the final points of jumps on the upper and lower stable branches of the SIM respectively. Still, such motion is possible only if the system can reach the fold lines $N_{1,2}$ while moving on the SIM with respect to the slow time scale. In order to assess this possibility, one should investigate the behavior of $\Phi(\tau_1)$. For this sake, we consider the ε^1 term of multiple-scale expansion, namely the second equation of (7). We are interested in the behavior of the solution on the stable branches of the SIM $\Phi(\tau_1) = \lim_{\tau_0 \to +\infty} \varphi_2(\tau_0, \tau_1)$. Taking the limit $\tau_0 \to \infty$ in the second equation of System (7) and taking into account the asymptotic stability of the points of the stable branches with respect to time scale τ_0, one obtains:

$$\frac{\partial}{\partial \tau_1}\left[\frac{\lambda\Phi}{2} + \frac{i\Phi}{2} - \frac{i}{2}|\Phi|^2\Phi\right] + \frac{1-\sigma}{4}|\Phi|^2\Phi + \left[\frac{\sigma}{4} + \frac{i\lambda(1-\sigma)}{4}\right]\Phi - \frac{iA_1}{4} = 0. \tag{14}$$

Equation (12) can be written in the more convenient form:

$$\left[\frac{\lambda}{2} - \frac{i}{2} + i|\Phi|^2\right]\frac{\partial\Phi}{\partial\tau_1} - \frac{i}{2}\Phi^2\frac{\partial\Phi}{\partial\tau_1} = G,$$
$$G = -\frac{1-\sigma}{4}|\Phi|^2\Phi - \left[\frac{\sigma}{4} + \frac{i\lambda(1-\sigma)}{4}\right]\Phi + \frac{iA_1}{4}. \tag{15}$$

By taking complex conjugate of (13), it is possible to extract the derivative $\frac{\partial\Phi}{\partial\tau_1}$:

$$\frac{\partial\Phi}{\partial\tau_1} = \frac{2[(\lambda - i + 2i|\Phi|^2)G + i\Phi^2G^*]}{\lambda^2 + 1 - 4|\Phi|^2 + 3|\Phi|^4}. \tag{16}$$

Splitting the variable Φ to modulus and argument $\Phi(\tau_1) = N(\tau_1)\exp(i\theta(\tau_1))$, one obtains the equations of the reduced flow in polar coordinates:

$$\begin{aligned}\frac{\partial N}{\partial\tau_1} &= \frac{-\lambda N - A_1N^2\cos\theta + \lambda A_1\sin\theta + A_1\cos\theta}{2(\lambda^2 + 1 - 4N^2 + 3N^4)},\\ \frac{\partial\theta}{\partial\tau_1} &= \big[(1-4\sigma)N^2 + \big(\sigma - \lambda^2(1-\sigma)\big)\\ &\quad - 3(1-\sigma)N^4 + 3A_1N\sin\theta\\ &\quad + A_1(\lambda\cos\theta - \sin\theta)/N\big]\\ &\quad \times\big[2\big(\lambda^2 + 1 - 4N^2 + 3N^4\big)\big]^{-1}.\end{aligned} \tag{17}$$

Denoting the numerators and denominator of the right hand side of system (15) by $f_1(N, \theta)$ for the first equation, $f_2(N, \theta)$ for the second equation and $g(N)$ for the denominator, system (15) is presented in the following form:

$$\frac{\partial N}{\partial\tau_1} = \frac{f_1(N,\theta)}{g(N)}, \qquad \frac{\partial\theta}{\partial\tau_1} = \frac{f_2(N,\theta)}{g(N)}. \tag{18}$$

Rescaling the time by the function $g(N)$ yields the equations for a "desingularized" flow:

$$N' = f_1(N, \theta), \qquad \theta' = f_2(N, \theta). \tag{19}$$

Regular points of the SIM are defined as those that satisfy the inequality $g(N) \neq 0$. The *fold lines* N_i, $i = 1, 2$ of the SIM are, by definition above, the sets of points (N, θ) where $g(N) = 0$.

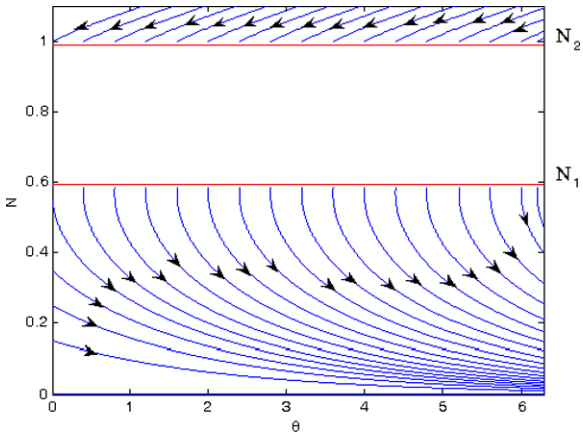

Fig. 2 Phase portrait of the slow invariant manifold for the case $A_1 = 0$, $\lambda = 0.2$, $\sigma = 0$

Let us start from particular case $A_1 = 0$. In this case, (15) are reduced to

$$\frac{\partial N}{\partial \tau_1} = \frac{-\lambda N}{2(\lambda^2 + 1 - 4N^2 + 3N^4)},$$
$$\frac{\partial \theta}{\partial \tau_1} = \frac{(1-4\sigma)N^2 + (\sigma - \lambda^2(1-\sigma)) - 3(1-\sigma)N^4}{2(\lambda^2 + 1 - 4N^2 + 3N^4)}. \tag{20}$$

Phase portrait of system (18) is presented at Fig. 2 (system parameters: $\lambda = 0.2$, $\sigma = 0$). Fold lines N_1, N_2 are marked on the phase portrait as dashed lines. It is clear from the first equation of (18), that the phase trajectories on the upper stable branch are directed toward the fold line, whereas the trajectories at the lower stable branch cannot bring the slow flow to the fold line. It means that the trajectory can "jump" from the upper stable branch to the lower one, but cannot jump back. It is trivial, since in the absence of forcing the system should be damped out.

In order to allow the jumps from the lower stable branch (and, therefore, to provide the necessary condition for the relaxation oscillations) the slow flow in the vicinity of the lower fold line should undergo some bifurcations. Namely, the N' value for some points on the lower fold should change sign from negative to positive one. Consequently, we can state that for some point or points on the lower fold the *normal switching condition* [19, 20] should be violated in the course of the bifurcation. In order to investigate this mechanism, we first compute the fixed points of the slow-flow equation (17) for arbitrary A_1.

Before, we proceed with the calculation of the equilibrium points of (17) let us define the two different types of these points. The first type is referred to as *ordinary fixed point*. These are equilibrium points of slow flow (17) which satisfy $N' = \theta' = 0$ and $g(N) \neq 0$. The second type is referred to as *folded singularities*. Folded singularities satisfy both $N' = \theta' = 0$ and $g(N) = 0$. They can be classified as equilibrium points of the two-dimensional flow (17) belonging to the fold lines.

Equilibrium points of the slow-flow system are found from (17) by setting both time derivatives equal to zero, thus providing

$$f_1(N, \theta) = 0,$$
$$f_2(N, \theta) = 0. \tag{21}$$

System (19) can be presented in the following matrix form:

$$\begin{pmatrix} \alpha_{11} & \alpha_{12} \\ \alpha_{21} & \alpha_{22} \end{pmatrix} \begin{pmatrix} \cos\theta \\ \sin\theta \end{pmatrix} = \begin{pmatrix} \beta_1 \\ \beta_2 \end{pmatrix}, \tag{22}$$

where

$$\alpha_{11} = \frac{1}{4}\lambda A_1; \qquad \alpha_{12} = -\frac{1}{4}A_1 + \frac{3}{4}N^2 A_1;$$
$$\alpha_{21} = \frac{1}{4}A_1 - \frac{1}{4}N^2 A_1; \qquad \alpha_{22} = \frac{1}{4}\lambda A_1;$$
$$\beta_1 = \frac{1}{4}N\sigma + \frac{1}{4}N^3 + \frac{1}{4}N\lambda^2\sigma - \frac{3}{4}N^5 - N^3\sigma - \frac{1}{4}N\lambda^2 + \frac{3}{4}N^5\sigma;$$
$$\beta_2 = -\frac{1}{4}N\lambda.$$

As was mentioned before, system (20) has two different types of solutions. The first type is obtained by solving (20) and assuming that the α matrix determinant does not vanish ($\alpha_{11}\alpha_{22} - \alpha_{21}\alpha_{12} \neq 0$). Thus the first type of solution is calculated from:

$$\left[\lambda^2 + \frac{\sigma^2}{(1-\sigma)^2}\right] N_0^2 + \frac{2\sigma}{1-\sigma} N_0^4 + N_0^6 = \frac{A_1^2}{(1-\sigma)^2}; \tag{23}$$
$$\theta_0 = \tan^{-1}\left(\frac{\sigma}{\lambda(1-\sigma)} + \frac{N_0^2}{\lambda}\right).$$

It is easy to derive that

$$\alpha_{11}\alpha_{22}-\alpha_{21}\alpha_{12}=\frac{A_1^2}{16}\left(1+\lambda^2-4N^2+3N^4\right)$$
$$=\frac{A_1^2}{32}g(N);$$

then nullification of $g(N)$ brings to the simultaneous nullification of $\alpha_{11}\alpha_{22}-\alpha_{21}\alpha_{12}$. Therefore, solution (21) describes the ordinary fixed points. This solution also coincides with the solution for fixed points of initial equation (5). This is rather obvious since fixed points of the global flow quite naturally belong to the slow invariant manifold.

The second type of solution obeys the following condition:

$$g(N)=3N^4-4N^2+1+\lambda^2=0$$
$$\Rightarrow\quad \alpha_{11}\alpha_{22}-\alpha_{12}\alpha_{21}=0. \tag{24}$$

Combination of (22) and (20) yields to the following equality:

$$\frac{\alpha_{11}}{\alpha_{21}}=\frac{\alpha_{12}}{\alpha_{22}}=\frac{\beta_1}{\beta_2}. \tag{25}$$

Second type of solution is generated by (22) and by one of the equations of (20) since another equation is satisfied automatically due to (23). Thus, picking the first equation of (20), one obtains the following solution for the folded singularities:

$$\Theta_{1,2}=\gamma_{01}\pm\cos^{-1}\frac{\lambda N_1}{A_1\sqrt{(1-N_1^2)^2+\lambda^2}},$$
$$\Theta_{3,4}=\gamma_{02}\pm\cos^{-1}\frac{\lambda N_2}{A_1\sqrt{(1-N_2^2)^2+\lambda^2}}, \tag{26}$$
$$\gamma_{0k}=\sin^{-1}\frac{\lambda}{\sqrt{(1-N_k^2)^2+\lambda^2}},\quad k=1,2.$$

The first pair of the folded singularities exists on the lower fold and is given by (N_1,Θ_1), (N_1,Θ_2). The second pair exists on the upper fold and is given by (N_2,Θ_3), (N_2,Θ_4). The first pair of the folded singularities exists if the following conditions hold:

$$\left|\frac{\lambda}{\sqrt{(1-N_k^2)^2+\lambda^2}}\right|\le 1, \tag{27a}$$

$$\left|\frac{\lambda N_1}{A_1\sqrt{(1-N_1^2)^2+\lambda^2}}\right|\le 1. \tag{27b}$$

Condition (27a) holds for arbitrary values of λ. However, condition (27b) holds only if

$$A_1\ge A_{11\mathrm{crit}}=\frac{\lambda N_1}{\sqrt{(1-N_1^2)^2+\lambda^2}}. \tag{28}$$

Similarly for the second pair of folded singularities the solvability condition reads

$$A_1\ge A_{12\mathrm{crit}}=\frac{\lambda N_2}{\sqrt{(1-N_2^2)^2+\lambda^2}}. \tag{29}$$

Therefore, it is easy to see that if the external forcing is relatively small,

$$A<A_{1\mathrm{crit}}=\frac{\lambda N_1}{\sqrt{(1-N_1^2)^2+\lambda^2}} \tag{30}$$

there are no folded singularities at the SIM. Consequently, the slow flow in the vicinity of both fold lines remains qualitatively similar to that on Fig. 2, providing no possibility of the relaxation oscillations.

In order to illustrate the qualitative changes in the reduced flow dynamics for the various forcing amplitudes we construct several phase portraits for the system (15). These phase portraits are plotted only for the case of single ordinary fixed point. It is convenient to pick zero frequency detuning $\sigma=0$. Only the flow at two stable branches of the SIM is presented. We start with the case $0<A_1<A_{11\mathrm{crit}}$ ($A_1=0.1$, $\lambda=0.2$).

An ordinary fixed point is marked on the phase portrait (lower stable branch of SIM) with rectangle. As becomes clear from the phase portrait of Fig. 3 there are no folded singularities for this case ($0<A_1<A_{11\mathrm{crit}}$) therefore we can see that all trajectories are finally attracted to the ordinary fixed point and there are no possibilities for relaxation oscillation. However, as the forcing approaches the value $A_1=A_{11\mathrm{crit}}$, the "saddle-node" bifurcation occurs at the lower fold line at $\theta=\gamma_{01}$. The phase portrait of the SIM for the case $A_{11\mathrm{crit}}<A_1<A_{12\mathrm{crit}}=\frac{\lambda N_2}{\sqrt{(1-N_2^2)^2+\lambda^2}}$, $A_1=0.18$ is presented on Fig. 4.

Phase portrait presented on Fig. 4 contains both ordinary fixed point on the lower branch of the SIM (marked with rectangle on the figure) and folded singularities (of saddle and node types). The region on

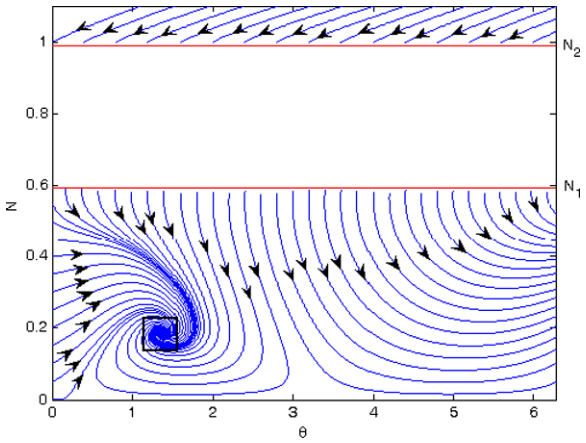

Fig. 3 Phase portrait of the slow invariant manifold for the case $0 < A_1 < A_{11\text{crit}}$ (only stable branches of the SIM are shown). System parameters: $A_1 = 0.1$, $\lambda = 0.2$, $\sigma = 0$. Ordinary fixed point is marked (on the lower stable branch of SIM) with *rectangle*

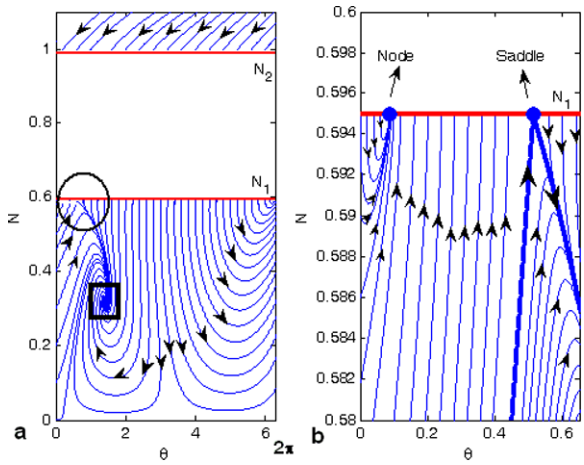

Fig. 4 (**a**) Phase portrait of the slow invariant manifold for the case $A_{11\text{crit}} < A_1 < A_{12\text{crit}}$ (only stable branches of the SIM are shown). System parameters: $A_1 = 0.18$, $\lambda = 0.2$, $\sigma = 0$. Ordinary fixed point is marked (on the lower stable branch of SIM) with *rectangle*. (**b**) Zoomed part of the phase portrait (marked with a *circle* on (**a**), which contains folded singularities (saddle and node)

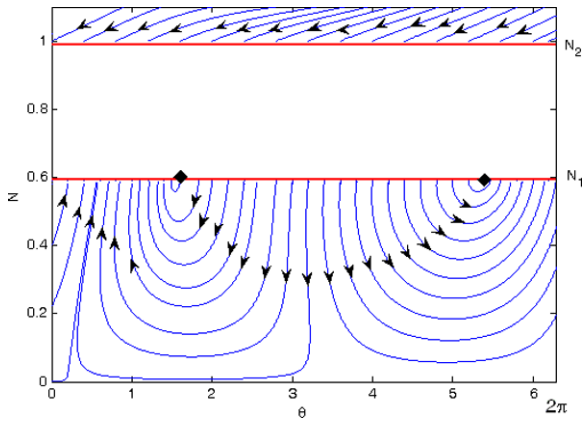

Fig. 5 Phase portrait of the slow invariant manifold for the case $0 < A_1 < A_{11\text{crit}}$ (only stable branches of the SIM are shown). System parameters: $A_1 = 0.5$, $\lambda = 0.2$, $\sigma = 0$. Ordinary fixed point is absent on the stable branches of SIM. Folded singularities are marked with *diamonds*

the phase portrait (Fig. 4a) bounded with a circle is zoomed and is illustrated on Fig. 4b. Folded singularities marked with the bold dots on the fold line are clearly observed on Fig. 4b. The trajectory which comes close to the separatrix of the saddle point is marked with the bold solid line.

The following phase portrait (Fig. 5) is drawn for the same region ($A_{11\text{crit}} < A_1 < A_{12\text{crit}}$, $A_1 = 0.5$) but for the increased value of forcing.

As we can see on Fig. 5 system dynamics undergoes some qualitative changes. It is important to emphasize that folded saddle propagates in the right direction along folded line and the folded node propagates in the left direction. The detailed study of the bifurcations of the folded singularities was carried out in [18].

Thus from Figs. 4 and 5 it is easy to see that once the bifurcations occur some phase trajectories on the SIM will bring the flow to the lower fold line $N = N_1$, thus providing a possibility for the jump to the upper stable branch. Then the flow can arrive to the upper fold line and jump down, thus closing the loop of the relaxation oscillation period referred in literature [17–21] as strongly modulated response (SMR). It is interesting to mention that the values of $A_{1\text{crit}}$ do not depend on the detuning parameter σ.

Still, from numerical simulations [16] it is known that these relaxation oscillations corresponding to strongly modulated response (SMR) exists only in comparatively narrow vicinity of exact 1:1 resonance between the external force and the natural frequency of the linear oscillator. It is clear therefore that the condition (24) is necessary, but by no means sufficient. In order to obtain the missing sufficient conditions, one should investigate more delicate details of the system dynamics.

The detailed study of the necessary and sufficient conditions for the existence of SMR regime was carried out in [18] via construction of one-dimensional

maps and will not be brought herein for the case of a single term excitation. In the following sections we bring the detailed analysis of the slow-flow dynamics on the SIM for the double term excitation case as well as construction of the 2D maps for studying the bifurcations of SMR.

2.2 Analysis of the slow-flow dynamics on the stable branches of SIM for the case of double term excitation ($A_2 > 0$)

We turn now to a systematic study of the full slow-flow equation derived for a double term excitation (4). Analysis of (4) is quite similar to the one for the case of single term excitation ($A_2 = 0$) and therefore only final derivations are presented.

It may be easily demonstrated from the analysis presented in the previous chapters that the structure of SIM itself is not affected by an addition of the second exciting force. This becomes apparent from the observation of the full slow-flow system (4). As one may notice all the external forcing parameters are of order $O(\varepsilon)$ and therefore in the previously brought multiple scales analysis can only affect the slow dynamics on the stable branches of SIM. The reduced slow-flow equation governing the motion on the stable branches of SIM for the double forcing case will yield:

$$\begin{aligned}
&\frac{\partial \Phi}{\partial \tau_1} = \frac{2[(\lambda - i + 2i|\Phi|^2)G + i\Phi^2 G^*]}{\lambda^2 + 1 - 4|\Phi|^2 + 3|\Phi|^4},\\
&G = -\frac{1-\sigma}{4}|\Phi|^2\Phi - \left[\frac{\sigma}{4} + \frac{i\lambda(1-\sigma)}{4}\right]\Phi\\
&\qquad + \frac{i(A_1 + A_2\exp(i\delta))}{4},\\
&\frac{\partial \delta}{\partial \tau_1} = \sigma_2.
\end{aligned} \tag{31}$$

As was already discussed in the previous subsection (for the single term excitation case $A_2 = 0$) there exist two possibilities for the flow depicted by reduced slow-flow analysis. The first possibility is to stay on one of the stable branches of SIM and to get attracted by one of the fixed point of either lower or upper stable branches. Apparently the second possibility is to exhibit consequent jumps from one stable branch to another. The first possibility corresponds to the trivial periodic-response regimes with constant amplitude when the second possibility is related to the SMR regime exhibited by the original system.

As was shown in the previous studies [17, 19, 21] of similar systems with single exciting harmonic term; these trivial periodic regimes are related to the regular fixed points of the upper stable branch of SIM and may be disadvantageous for vibration mitigation. In fact, these regimes bring about rather high-amplitude oscillations of the primary mass, which is supposed to be protected.

One of the possibilities to eliminate these responses is to constantly perturb the system near these stable fixed points of the upper stable branch of SIM in order to cause it to jump down to the lower stable branch. If there is another fixed point on the lower stable branch the phase trajectory has a possibility to be attracted to this fixed point or to perform another relaxation back to the upper stable branch. Thus, the system trajectory is left with only two possibilities of either being attracted by a certain stable attractive set of the lower stable branch or to perform consequent relaxation jumps. Both possibilities are favorable in a sense of vibration suppression [17, 19, 21]. If one assumes relatively small additional forcing A_2 and linearizes (31) near a regular fixed point, one will obtain approximate linear system with constant harmonic forcing. This will result in limit cycles on the stable branches of SIM encircling the fixed points of the upper stable branches. Apparently these limit cycles will grow with the increasing A_2. It is also clear that all these trajectories of the limit cycles may exist only if they do not collide with one of the fold lines. Therefore, increasing the amplitude of the limit cycle slightly above certain threshold will result in the relaxation jump to the lower stable branch. This also means that no stable attractors on the upper stable branch will exist and thus only the favorable responses will remain in the system.

As one may easily observe, system (31) contains a time dependent term which means that the reduced system (5) is not autonomous anymore and hence its state space has dimensionality higher than 2. This also means that we cannot proceed with the straightforward studying of the complete phase portraits. In the present work we restrict our attention to study of the aforementioned limit cycles on the stable branches of SIM; the latter encircle the regular fixed points corresponding to $A_2 = 0$. Numerical examples are presented at Figs. 6a and 6b. Limit cycles of Fig. 6a are the steady-state solutions of (5) on the upper stable branch and those of Fig. 6b correspond to the lower one. For sufficiently small values of A_2 those limit cycles exist on

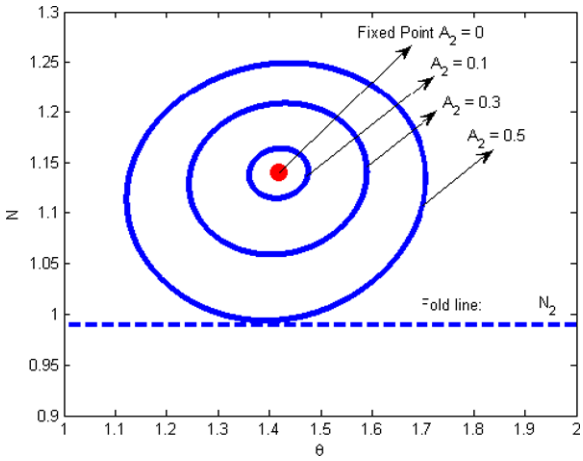

Fig. 6a Limit cycles created on the upper branch of SIM for $(A_2 = 0, 0.1, 0.3, 0.5)$; the rest system parameters are $A_1 = 1.5$, $\lambda = 0.2$, $\sigma = 0$, $\sigma_2 = 0.1$

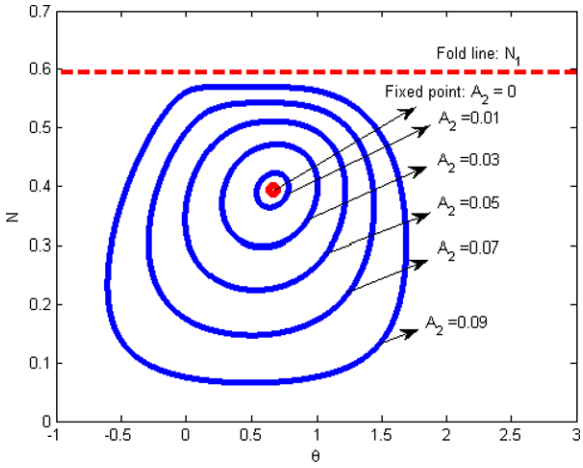

Fig. 6b Limit cycles created on the lower branch of SIM for $(A_2 = 0, 0.01, 0.03, 0.05, 0.07, 0.09)$; the rest system parameters are $A_1 = 0.1$, $\lambda = 0.2$, $\sigma = 0$, $\sigma_2 = 0.1$

the stable branches of SIM and are encircling the regular fixed points corresponding to the autonomous system $(A_2 = 0)$.

It is clear from Figs. 6a, 6b that as the amplitude of the second forcing term is increased the radius of the limit cycles is constantly growing. Rather obvious criterion for the existence of the limit cycles and their annihilation may be established.

Let us denote the regular fixed point of the corresponding autonomous system $(A_2 = 0)$ by Φ_0 and the set of all points on the limit cycles of the stable branches of SIM by $\gamma(\tau_1) = R(\tau_1)\exp(i\vartheta(\tau_1)) + \Phi_0$.

Conditions for the existence of a stable limit cycle on the stable branches of SIM may be formulated as follows:

1. $|\Phi_0| \in \{x \mid 0 < x < N_1, N_2 < x\}$;
2. $\forall \vartheta(\tau_1) \in [0, 2\pi]$,
$$R(\tau_1) < \big||\Phi_0| - N_2\big|, \quad |\Phi_0| > N_2, \tag{32}$$
$\forall \vartheta(\tau_1) \in [0, 2\pi]$,
$$R(\tau_1) < \big||\Phi_0| - N_1\big|, \quad |\Phi_0| < N_1.$$

If the two conditions are not satisfied simultaneously then one would expect for any stable limit cycle on the stable branches of SIM. In fact the first condition of (32) requires for the regular fixed point of the autonomous system to be situated at least on one of the stable branches of SIM (not including the fold lines). The second condition is rather naïve since it requires for the entire set of the points of a limit cycle to belong completely to the stable branches of SIM. However if the limit cycle hits the fold lines of the SIM, then, obviously, the phase trajectories escape from the stable branches and the stable limit cycle ceases to exist. This point should be explained in details in order to avoid possible ambiguity of definitions. When we say that limit cycles cease to exist we refer to the particular family of limit cycles localized on the stable branches of SIM. However, as is clear from the previous discussions there can exist another family of limit cycles which is not localized to a single branch of SIM and is characterized by successive jumps from one stable branch to another. At this point it would be appropriate to make a classification of the two distinct families of limit cycles. The first family of localized limit cycles (their trajectories may be shrinked into a point by gradually decreasing A_2) refers to the weakly modulated responses. The second family is related to a SMR regime.

Analytical approximation of the limit cycles of the first type can be derived by linearization around regular fixed points. Thus small deviations around a regular fixed point of an autonomous system $(A_2 = 0)$ are introduced as follows:

$$\Phi(\tau_1) = \Phi_0 + \xi(\tau_1), \quad |\xi| \ll |\Phi_0|. \tag{33}$$

Here we also assume that the magnitude of the additional harmonic force A_2 is of the same order as $\xi(\tau_1)$.

Substituting (33) into (31) and collecting the terms of the first order yields the following linear system:

$$\begin{aligned}\frac{d\xi}{d\tau_1} &= \alpha_{11}(\Phi_0,\Phi_0^*)\xi + \alpha_{12}(\Phi_0,\Phi_0^*)^*\xi^* \\ &\quad + \beta_1(\Phi_0,\Phi_0^*)\exp(i\sigma_2\tau_1) \\ &\quad + \beta_2(\Phi_0,\Phi_0^*)\exp(-i\sigma_2\tau_1), \\ \frac{d\xi^*}{d\tau_1} &= \alpha_{11}(\Phi_0,\Phi_0^*)^*\xi^* + \alpha_{12}(\Phi_0,\Phi_0^*)^*\xi \\ &\quad + \beta_1(\Phi_0,\Phi_0^*)^*\exp(-i\sigma_2\tau_1) \\ &\quad + \beta_2(\Phi_0,\Phi_0^*)^*\exp(i\sigma_2\tau_1).\end{aligned} \tag{34}$$

The full expressions for $\alpha_{11}, \alpha_{12}, \beta_1, \beta_2$ are presented in Appendix. It is convenient to rewrite (34) in a matrix form:

$$\frac{d\underline{\xi}}{dt} = \underline{B}\underline{\xi} + \underline{F}(\tau_1) \tag{35}$$

where

$$\underline{\xi} = \begin{pmatrix}\xi \\ \xi^*\end{pmatrix}, \qquad \underline{B} = \begin{pmatrix}\alpha_{11} & \alpha_{12} \\ \alpha_{11}^* & \alpha_{12}^*\end{pmatrix},$$

$$\underline{F}(\tau_1) = \begin{pmatrix}\beta_1(\Phi_0,\Phi_0^*)\exp(i\sigma_2\tau_1) + \beta_2(\Phi_0,\Phi_0^*)\exp(-i\sigma_2\tau_1) \\ \beta_1(\Phi_0,\Phi_0^*)^*\exp(-i\sigma_2\tau_1) + \beta_2(\Phi_0,\Phi_0^*)^*\exp(i\sigma_2\tau_1)\end{pmatrix}$$

The system (35) possesses the well-known solution:

$$\underline{\xi}(\tau_1) = \underline{c\Psi}(\tau_1) + \underline{\Psi}(\tau_1)\int \underline{\Psi}^{-1}(\tau_1)\underline{F}(\tau_1)\,d\tau_1, \tag{36}$$

where: $\underline{\Psi}(\tau_1)$ is a matrix of fundamental solutions of a corresponding homogeneous system.

Comparison of the steady-state solutions of (36) and those of (4) is presented in Figs. 7a, 7b for upper and lower branches respectively.

As it is evident from the results of Figs. 7a, 7b analytical approximation becomes cruder with the growing values of the amplitude of a weak limit cycle. However, the earlier formulated conditions (32) necessary for the existence of weak limit cycles bring about the possibility of predicting threshold values of $A_{2\mathrm{TH}}$ beyond which no weak limit cycles are possible and therefore global flow is forced to the alternating jumps between the two stable branch surfaces. The latter type of motion is referred to as an aforementioned strongly modulated response regime (SMR).

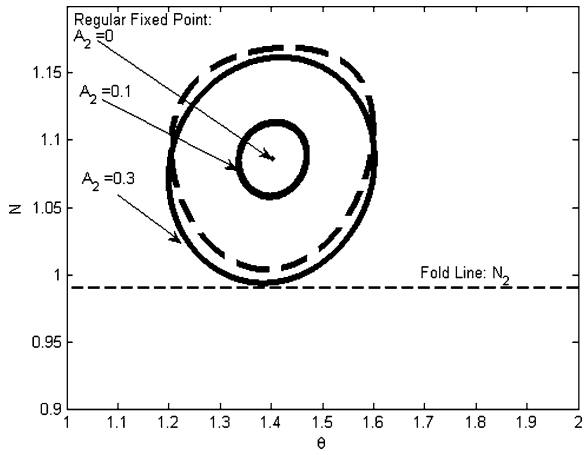

Fig. 7a Comparison of an analytical approximation of weak limit cycle on the upper stable branch with the numerical solution of (5). The *dashed line* relates to an analytical approximation; the *solid line* relates to numerical solution of (5). System parameters: $A_1 = 1.3$, $\lambda = 0.2$, $\sigma = 0$, $\sigma_2 = 0.1$

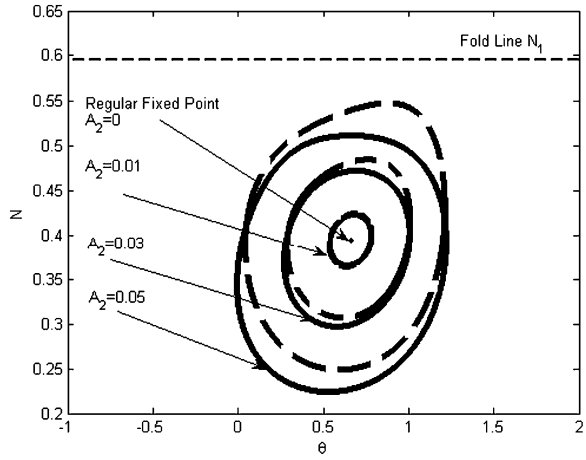

Fig. 7b Comparison of an analytical approximation of weak limit cycle on the lower stable branch with the numerical solution of (4). The *dashed line* relates to analytical approximation; the *solid line* relates to numerical solution of (4). System parameters: $A_1 = 0.1$, $\lambda = 0.2$, $\sigma = 0$, $\sigma_2 = 0.1$

2.3 Two-dimensional maps construction for a double term excitation ($A_2 > 0$)

In the present subsection we develop a semi-analytical approach based on the two-dimensional maps construction for finding special attractors of SMR and their bifurcations for the case of a double term excitation. As we have already noted in the previous sections in the regime of relaxation oscillations, the phase trajectory jumps from the lower fold to the upper branch

of the SIM, then it moves along the line of the slow flow until it hits again the upper fold line, then jumps back to the lower stable branch of SIM and moves toward the lower fold. The particular moment of the secondary piercing of the lower fold line by the trajectory (initially started from the lower fold line) corresponds to the completion of exactly one cycle by the SMR. Thus, as will be shown below, recording the phase space points (of the reduced order slow-flow model) of consequent piercings of the lower fold line by the trajectory in the regime of SMR makes it possible to recover stable attractors of the SMR regime and to follow their possible bifurcations-systematically. Unlike the case of a single harmonic term excitation the reduced slow-flow model system (5) derived for a double term excitation is non-autonomous and therefore the dimensionality of the resultant map will increase.

Let us start the description of the construction of the map for the SMR cycles from the definition of the cross-section. We choose the lower fold ($N = N_1$) as a section of the map. As is clear from the analysis of previous subsection each point of the phase space describe by the reduced order, slow-flow model (31) is uniquely defined by Φ, δ. Thus rewriting Φ in a polar form as:

$\Phi = N\exp(i\theta)$ we formally define the section of the map as follows,

$$\Sigma = \left\{|\Phi| = N_1\right\} \cap \{-\pi < \theta < \pi\} \cap \left\{\delta \bmod (2\pi)\right\}. \tag{37}$$

Thus the map will be defined as $P : \Sigma \to \Sigma$. The idea of constructing maps for the trajectories reaching the lower fold line was developed earlier in [18] for the case of single exciting term $A_2 = 0$. However, the previously developed maps were one-dimensional and an interval between the two folded singularities of the lower fold line was defined as the section of the map. All the trajectories that left the lower branch (were not attracted to any other stable attractor of the lower branch) have pierced this interval (see [18] for details). In the present paper we follow the same idea of using the lower fold line as a section of mapping, however it is clear that section (37) is two-dimensional, due to the addition of time dependent forcing in the reduced slow-flow system (31). This also means that we have no convenient restrictions on the section interval as it was in the single term excitation case $A_2 = 0$, this is why the section (37) by definition includes the entire domain.

The function P of the defined two-dimensional map (37) is calculated semi-analytically. In order to construct the relevant map, we should consider separately the "slow" and the "fast" parts of the mapping cycle. As for the "slow" parts on the lower and the upper branches of the SIM, we can use (4) and directly connect the "entrance" and "exit" points. Due to the complexity of the equations, this part of the mapping should be accomplished numerically. As for the "fast" parts, the function Φ should be continuous at the points of contact between the "fast" and the "slow" parts. Therefore, for "fast" parts of the motion one obtains complex invariant $C(\tau_1)$, defined by (10). It is important to note that there is a place for possible confusion since (10) corresponds to the part of analysis developed for a single term excitation case. However, as one may notice directly from (8), (9), (10) that none of the external excitation terms (A_1, A_2) enter the equation in the zero order approximation (derived for a fast time scale) and therefore (10) originally derived for a single excitation term will be also valid for the double excitation case.

Thus if one knows its value at the point of "start" on the section Σ, it is possible to compute N and θ for the point of "finish" unambiguously. As for the value of δ in the point of 'finish' on the upper stable branch one may easily see from the previous analysis that δ is a slow time scale variable and therefore remains unchanged (in the singular limit!) during the fast relaxation.

The procedure of numerical integration should be performed twice-for two branches of the SIM. Two invariants should be computed for two "fast" jumps, in order to determine their final points. It should be stressed that only one computation cycle of the mapping for each point of the initial domain is required.

In general, not every trajectory which starts from the lower fold of the SIM will reach the initial starting section Σ since it may be attracted to alternative attractor at the upper or the lower branch of the SIM, if it exists. Of course, only those points which are mapped into the initial domain, can carry sustained relaxation oscillations and are of interest in scope of the current paper. The schematic construction of the return map is illustrated at Fig. 8. Thus, starting from some initial point on section Σ one may compute the finite set of consequent mappings $P^N : \Sigma \to \Sigma$. Moreover we would like to point out that in the scope of the current paper we are solely interested in finding attractors of the SMR regime, hence in the following

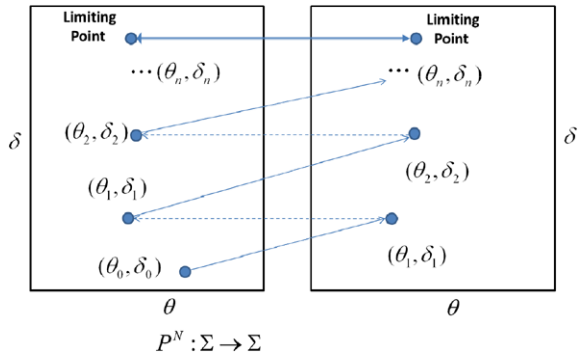

Fig. 8 Schematic construction of the return map. (θ_0, δ_0) is an initial guess, (θ_n, δ_n) a limiting point

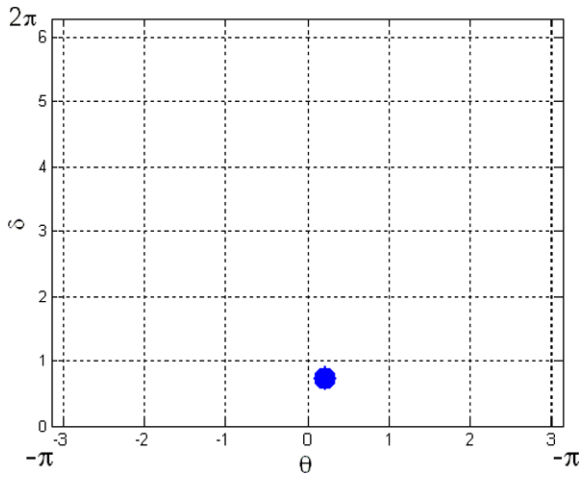

Fig. 9a Single periodic attractor captured by two-dimensional map procedures. System parameters: $A_1 = 0.1$, $A_2 = 0.2$, $\sigma_1 = 0, \sigma_2 = 1$

two-dimensional maps we skip the initial mappings (i.e. $(\theta_0, \delta_0), (\theta_1, \delta_1), \ldots, (\theta_{n-1}, \delta_{n-1})$) and plot only the final periodic attractors/invariant sets of the SMR to which the series of mappings converge (see the schematic example of a one-period attractor illustrated on Fig. 8).

Example of 2D maps construction for some particular values of system parameters is illustrated in Figs. 9a–9c. In this example we fix the value of the amplitude $A_1 = 0.1$ and vary the value of the second amplitude A_2.

As one may observe from the results of Figs. 9a–9c the 2D maps undergo qualitative bifurcations as the value of the second exciting term amplitude is increased. At the relatively low value of the second exciting force amplitude ($A_2 = 0.2$) a single one-period

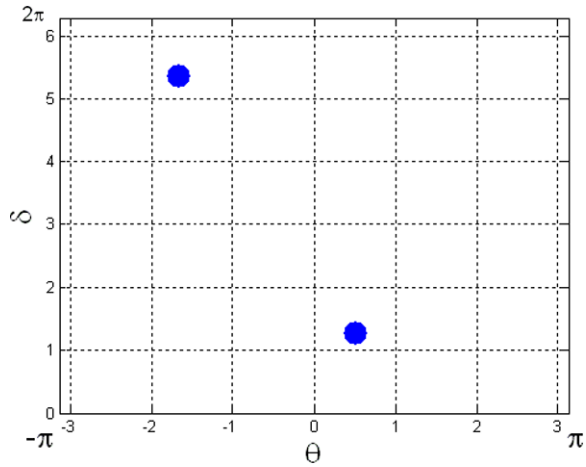

Fig. 9b Double periodic cycles captured by two-dimensional map procedure. System parameters: $A_1 = 0.1$, $A_2 = 0.7$, $\sigma_1 = 0, \sigma_2 = 1$

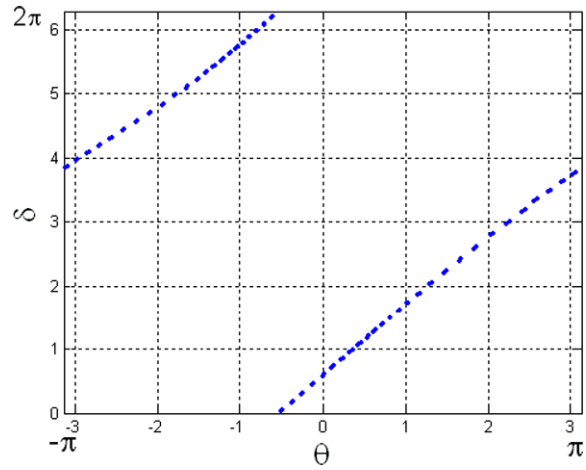

Fig. 9c Invariant set captured by two-dimensional map procedure. System parameters: $A_1 = 0.1$, $A_2 = 0.9$, $\sigma_1 = 0, \sigma_2 = 1$

attractor may be observed for the SMR regime. As the value of the second forcing amplitude becomes higher, then there is a period doubling bifurcation As becomes clear from Fig. 9b. Increasing the value of A_2 above additional threshold the map recovers another invariant set (Fig. 9c). The latter observation of the invariant set may be regarded as a phase unlocking between the forcing phase and the phase of the response (SMR) in terms of the two-dimensional mapping. It is worthwhile noting that no Feigenbaum cascade (over the two periodic cycles) was observed in the parametric scanning of rather high resolution. Apparently this means that the system under investigation

deserves additional study for gaining more rigorous and complete understanding of the bifurcation structure observed herein.

3 Numerical simulations

3.1 Numerical verifications of the theoretical model

In the present section we are willing to provide numerical confirmation for the analytically predicted phenomena of the birth of weak limit cycles for some law amplitudes of the second exciting term (A_2) and their bifurcations due to the increase in the amplitude leading to the excitation of the relaxation-type motions referred to as SMR regime. Before we proceed with the numerical verifications of the semi-analytically predicted behavior on the stable branch of SIM we plot the limit cycles of (5) (Fig. 10) on the upper branch of SIM corresponding to the system parameters chosen for the further numerical simulations. System parameters chosen for the simulations are as follows; $A_1 = 1.3$, $\lambda = 0.2$, $\varepsilon = 0.01$, $\sigma = 0$, $\sigma_2 = 1$, A_2 parameter is varied in the simulations. As one may observe from the results of Fig. 10 weak limit cycles exist on the upper stable branch for the limited range of A_2 parameter ($0 < A_2 < 0.19$).

Let us first start with the validations of the simple periodic-response regimes corresponding to the fixed points on the stable branches of SIM for the case of a single exciting term (i.e. $A_2 = 0$) (Fig. 11).

Time series of relative displacement between the linear oscillator and the NES are illustrated in Fig. 11 for the single forcing case ($A_2 = 0.0$). Initial conditions for all the numerical simulation have been chosen in correspondence with a regular fixed point on the upper branch of SIM. Steady-state solution for the slow flow on SIM is also plotted. Fairly good agreement between the analytical model and numerical simulation of the original system (1) is observed. Interestingly enough would be to validate the change in the response of the original system with amplitude of the second exciting term below the predicted threshold ($A_2 < A_{2\text{CRITICAL}}$). Next simulation was performed for the following set of system parameters: $A_1 = 1.3$, $A_2 = 0.1$, $\lambda = 0.2$, $\varepsilon = 0.01$, $\sigma = 0$, $\sigma_2 = 1$. The predicted threshold (for this particular set of system parameters) beyond which the bifurcation of weak limit cycles occurs is: $A_{2\text{CRITICAL}} \approx 0.19$. Time series of relative displacement is illustrated along with the steady-state solution for the slow flow on SIM. Again spectacular agreement of the results of numerical simulation and analytical model (5) is evident from the results of Fig. 12.

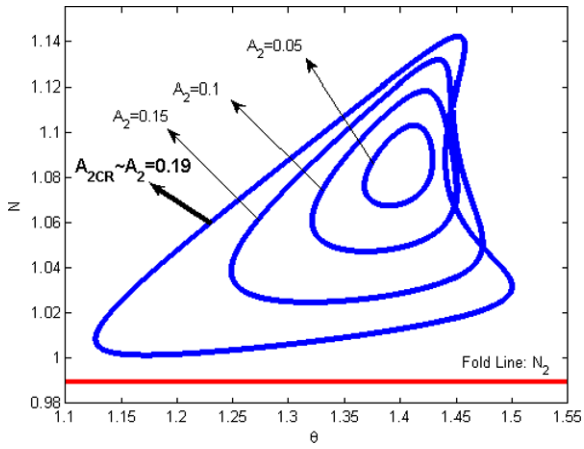

Fig. 10 Limit cycles of the slow flow on upper branch of SIM corresponding to (5). System parameters: $A_1 = 1.3$, $\lambda = 0.2$, $\sigma = 0$, $\sigma_2 = 1$

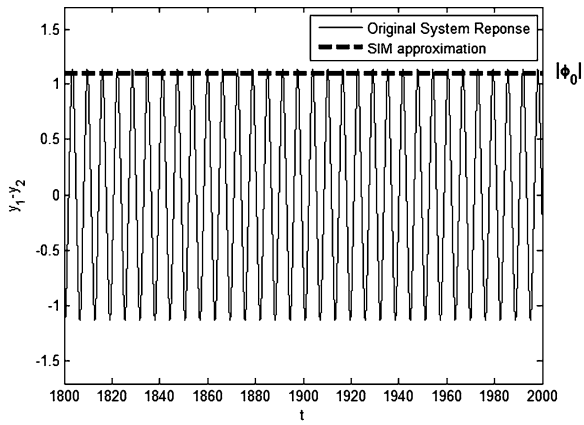

Fig. 11 Time series of a simple periodic-response regime related to a regular stable fixed point of the upper branch of SIM. Steady-state solution for the slow flow on SIM (5) is denoted by a *dashed line*. Corresponding numerical solution of an original System (1) is denoted by a *thin curve*. System parameters: $A_1 = 1.3$, $A_2 = 0.0$, $\lambda = 0.2$, $\varepsilon = 0.01$, $\sigma = 0$

The next simulation (Fig. 13) was performed for an amplitude value A_2 higher than the predicted threshold ($A_2 = 0.3 > A_{\text{cr}} = 0.19$) the rest system parameters are left the same.

As one may observe from the last simulation; beyond the predicted threshold of A_2—weak limit cycles are annihilated and SMR regime is excited and is

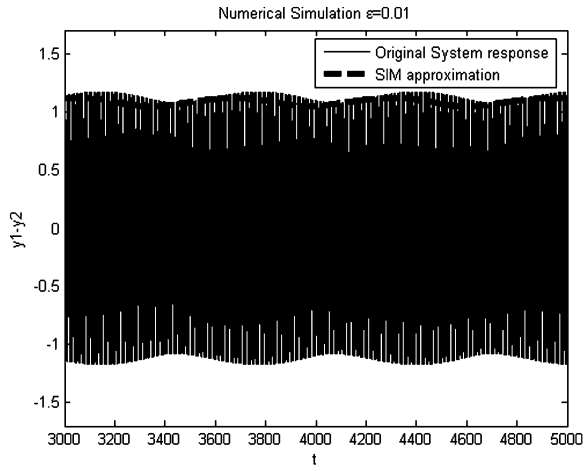

Fig. 12 Time series of a weakly modulated response regime related to a weak stable limit cycle of the upper branch of SIM (see Figs. 8a, 9a). Steady-state solution for the slow flow on SIM (5) is denoted by a *dashed line*. Corresponding numerical solution of an original System (1) is denoted by a *thin curve*. System parameters: $A_1 = 1.3$, $A_2 = 0.1$, $\lambda = 0.2$, $\varepsilon = 0.01$, $\sigma = 0$, $\sigma_2 = 1$

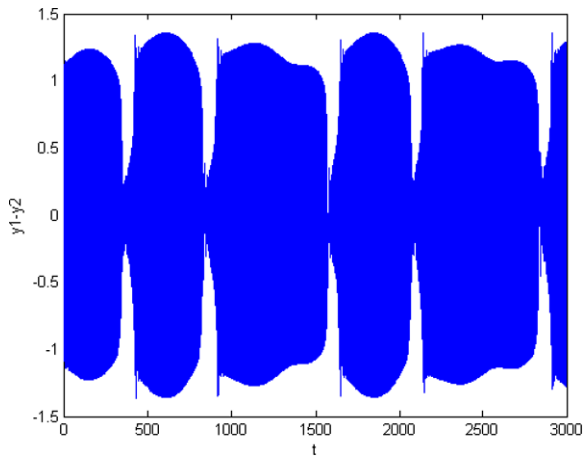

Fig. 13 Time series of the excited SMR regime $A_1 = 1.3$, $A_2 = 0.3$, $\lambda = 0.2$, $\varepsilon = 0.01$, $\sigma = 0$, $\sigma_2 = 1$

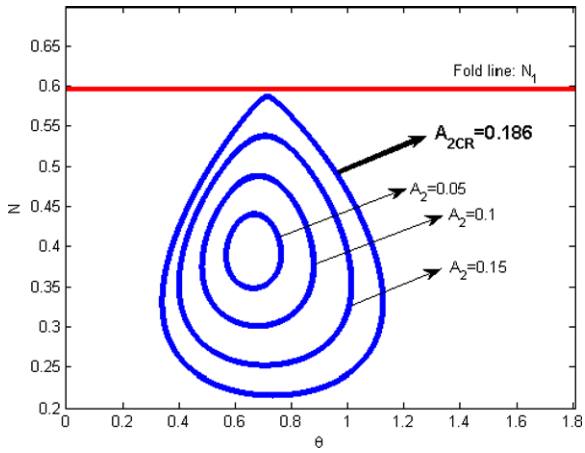

Fig. 14 Limit cycles of the slow flow on the lower branch of SIM corresponding to (5). System parameters: $A_1 = 0.1$, $\lambda = 0.2$, $\sigma = 0$, $\sigma_2 = 1$

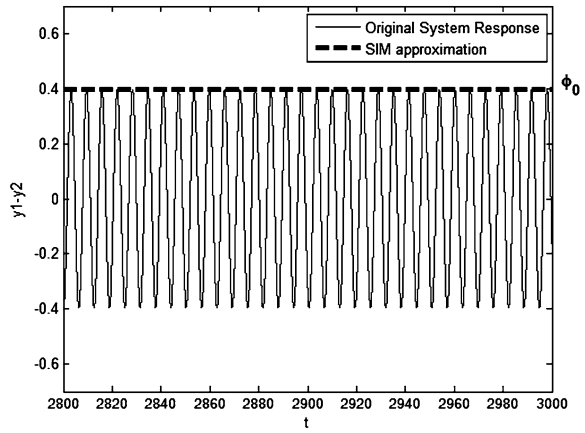

Fig. 15 Time series of a simple periodic-response regime related to a regular stable fixed point of the upper branch of SIM. Steady-state solution for the slow flow on SIM (5) is denoted by a *dashed line*. Corresponding numerical solution of an original System (1) is denoted by a *thin curve*. System parameters: $A_1 = 1.3$, $A_2 = 0.0$, $\lambda = 0.2$, $\varepsilon = 0.01$, $\sigma = 0$, $\sigma_2 = 1$)

characterized by the alternating jumps from one stable branch of SIM to another.

Similar numerical verification as for the slow-flow limits cycles of the upper stable branch of SIM is performed for the lower one. To this extent we plot again the limit cycles of slow flow (5) on the lower stable branch of SIM (Fig. 14). As one may observe from the results of Fig. 14, weak limit cycles exist on the lower stable branch for the limited range of A_2 parameter ($0 < A_2 < 0.19$).

Similar numerical simulations are performed to validate the predictions on the lower stable branch of the SIM. Again we start with a single forcing case $A_2 = 0$ (Fig. 15). The rest system parameters are as follows: $A_1 = 0.1$, $\lambda = 0.2$, $\sigma = 0$, $\sigma_2 = 1$, $\varepsilon = 0.01$.

The predicted threshold (for this particular set of system parameters) beyond which the bifurcation of weak limit cycles occurs is: $A_{2\mathrm{CRITICAL}} \approx 0.186$. Time series of relative displacement is illustrated along with the steady-state solution for the slow flow on SIM. Again spectacular agreement of the results of

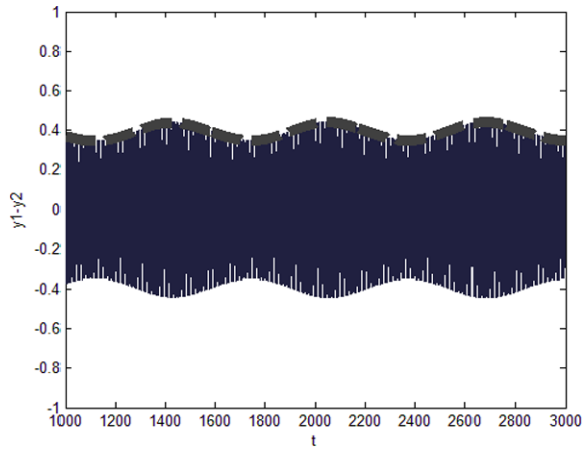

Fig. 16 Time series of a weakly modulated response regime related to a weak limit cycle of the upper branch of SIM (see Fig. 14). Steady-state solution for the slow flow on SIM (5) is denoted by a *dashed line*. Corresponding numerical solution of an original System (1) is denoted by a *thin curve*. System parameters: $A_1 = 0.1$, $A_2 = 0.05$, $\lambda = 0.2$, $\varepsilon = 0.01$, $\sigma = 0$, $\sigma_2 = 1$

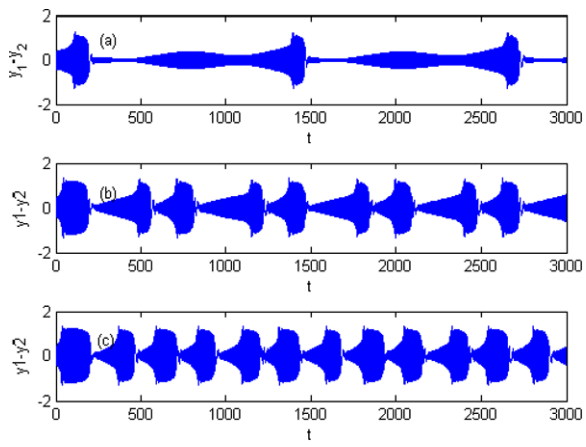

Fig. 17 Time series of SMR response regime for the values of the second exciting term amplitude—higher than threshold $A_{cr} = 0.186$, (**a**) $A_2 = 0.2$ (**b**) $A_2 = 0.7$ (**c**) $A_2 = 0.9$. The rest system parameters: $A_1 = 0.1$, $\lambda = 0.2$, $\varepsilon = 0.01$, $\sigma = 0$, $\sigma_2 = 1$

numerical simulation and analytical model (5) is evident from the results of Fig. 15.

The next simulation (Fig. 17a–17c) was performed for the amplitude values A_2 higher than the predicted threshold ($A_2 = 0.2, 0.7, 0.9 > A_{cr} = 0.186$) the rest system parameters are left the same.

It is important to note that system parameters chosen for the last simulations of SMR regime (Fig. 15) are not arbitrary and correspond to those picked for the two-dimensional maps example of previous section. As is evident from the example of two-dimensional maps, the mapping procedure predicts single SMR cycle for $A_2 = 0.2$, period doubling for $A_2 = 0.7$ and finally phase 'unlocking' for $A_2 = 0.9$. As may be observed from the results of Fig. 17 the predicted bifurcations are in agreement with the numerical simulations.

3.2 System response to a random narrow-band excitation

In the previous sections we provided analytical and numerical study of the system (1) subject to deterministic, quasi-periodic (weakly modulated) excitation. There we have found that above a certain limit of the amplitude of modulation of the incoming signal all the unpleasant, weakly quasi-periodic regimes may be successfully annihilated and the SMR regime is excited. The next question we would like to address numerically is whether randomly modulated, narrow-band excitation may cause the same effect of the complete elimination of undesired response and an alternative excitation of the SMR-like relaxation cycles.

This random excitation is defined as follows:

$$F(t) = \varepsilon A_1 \cos(t) + \varepsilon A_2 \cos\big(t + \gamma W(t)\big), \tag{38}$$

where A_1, A_2 are deterministic amplitudes, $W(t)$ is a standard Wiener process and $\gamma \geq 0$ is a bandwidth of the random excitation. Apparently for the purposes of narrow-band excitation γ is assigned rather small values. If A_2 is essentially less than A_1, the random modulation of the exciting force defined in (38) can still be regarded as weak.

In the present numerical study we are interested in studying the system response for the case of random amplitudes of modulation below the threshold ($A_2 < A_{2\text{threshold}}$) (where according to the previous results of deterministic amplitude-modulated excitation only weak limit cycles were excited) as well as above the threshold $A_2 > A_{2\text{threshold}}$. The following system parameters were chosen for the first numerical simulation:

$$A_1 = 1.3, \qquad A_2 = 0.1, \qquad \lambda = 0.2,$$
$$\gamma = 0.1, \qquad \varepsilon = 0.05.$$

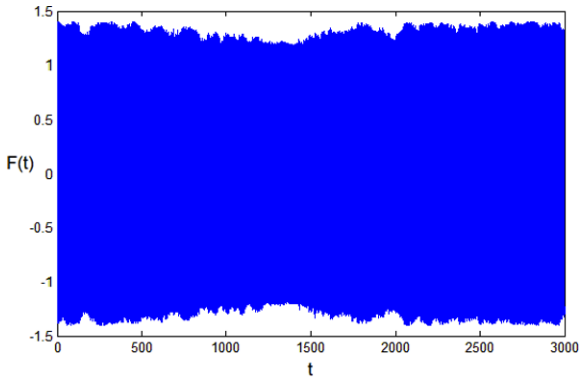

Fig. 18 Random forcing input realization. System parameters: $A_1 = 1.3$, $A_2 = 0.1$, $\lambda = 0.2$, $\gamma = 0.1$, $\varepsilon = 0.05$

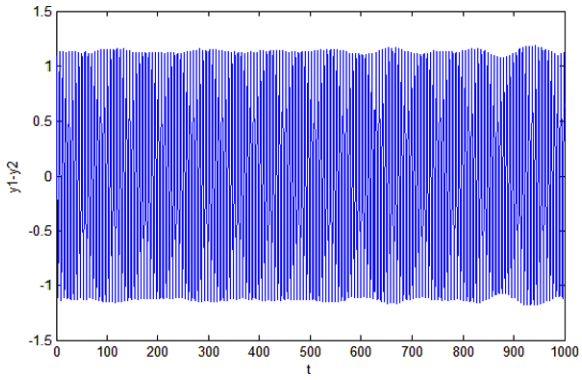

Fig. 19 Time series of the system (1) response to the external random excitation of Fig. 18

Two realizations of Wiener process were generated. The first realization was generated for the lower amplitude of $A_2 = 0.1$. The first random input for the first realization is illustrated on Fig. 18.

Time series of the response of System (1) to the first input realization (Fig. 18) is presented in Fig. 19.

As becomes clear from the results of Fig. 19 only weak modulation may be observed (no bursts related to a SMR regime).

In the next simulation we increase the value of the second term amplitude $A_2 = 0.5$. The following system parameters were chosen for the second numerical simulation $A_1 = 1.3$, $A_2 = 0.1$, $\lambda = 0.2$, $\gamma = 0.1$, $\varepsilon = 0.05$.

The second realization was generated for the higher amplitude of $A_2 = 0.5$. The second random forcing input for the second realization is illustrated on Fig. 20.

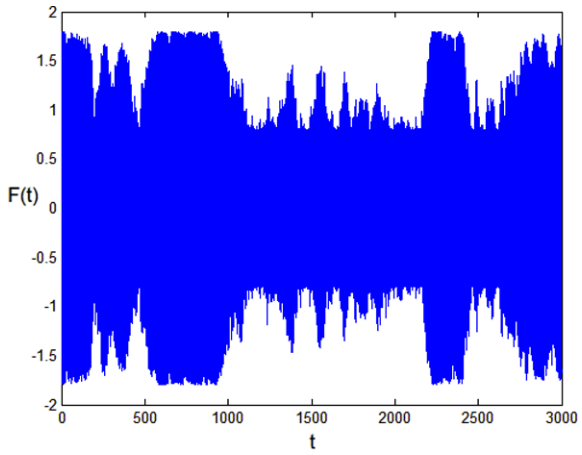

Fig. 20 Random forcing input realization. System parameters: $A_1 = 1.3$, $A_2 = 0.5$, $\lambda = 0.2$, $\gamma = 0.1$, $\varepsilon = 0.05$

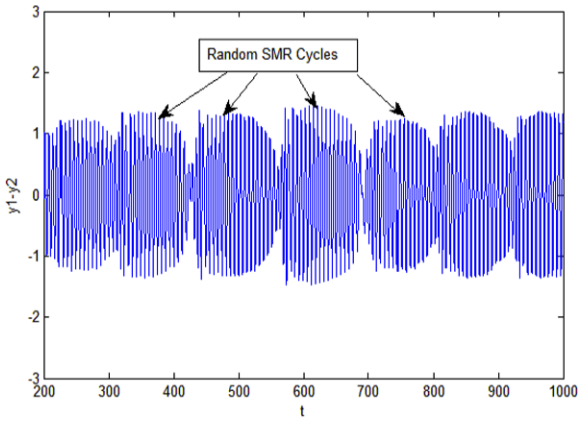

Fig. 21 Time series of the system (1) response to the external random excitation of Fig. 20

Time series of the response of System (1) to the second forcing input realization (Fig. 20) is presented in Fig. 21.

It is clear from the results of Fig. 21 that strongly modulated, random beats are excited for higher value of second exciting term amplitude. However, theoretical prediction of a threshold value above which strongly modulated beats are excited for the case of narrow-band random excitation is beyond the scope of the present paper and will be published elsewhere.

4 Concluding remarks

Main conclusion from the results presented above is that by adding relatively small excitation with close

frequency or random narrow-band signal, one can obtain rather strong modification of the response regimes in the forced system with the NES. This result is not totally unexpected, but the semi-analytic procedure presented here allows one to predict such modification and to design the system accordingly. In the context of the absorption of the vibration, the amplitude of additional signal necessary to eliminate the undesired response regimes can be not so small. Still, no optimization in any sense was performed in the paper, so one can hope to enhance these results by using more efficient NES [21]. From the other side, the paper demonstrates in the first time that one can devise the NES parameters in order to mitigate efficiently the multi-frequency and even random external excitations.

Acknowledgements The authors are very grateful to US—Israel Binational Science Foundation (grant 2008055) for financial support.

Appendix

$$\begin{aligned}
\alpha_{11} &= -\Big((\varphi_0^* - \varphi_0)A_1 + \frac{1}{2}i\lambda^2(1-\sigma) + \frac{1}{2}\lambda \\
&\quad + 4i(\sigma-1)|\varphi_0|^2 - \frac{1}{2}i\sigma + \frac{9}{2}i(1-\sigma)|\varphi_0|^4 \Big) \\
&\quad \times \left(1+\lambda^2 - 4|\varphi_0|^2 + 3|\varphi_0|^4\right)^{-1} \\
\alpha_{12} &= -\frac{(2i\sigma\varphi_0^2 + A_1\varphi_0 + 3i(1-\sigma)|\varphi_0|^2\varphi_0^2 - \frac{1}{2}i\varphi_0^2)}{1+\lambda^2 - 4|\varphi_0|^2 + 3|\varphi_0|^4}, \\
\beta_1 &= \frac{2iA_2(\lambda - i + 2i|\varphi_0|^2)}{4(1+\lambda^2 - 4|\varphi_0|^2 + 3|\varphi_0|^4)}, \\
\beta_2 &= \left(\frac{2A_2\varphi_0^2}{4(1+\lambda^2 - 4|\varphi_0|^2 + 3|\varphi_0|^4)} \right).
\end{aligned} \tag{A.1}$$

References

1. Gendelman, O.V.: Transition of energy to nonlinear localized mode in highly asymmetric system of nonlinear oscillators. Nonlinear Dyn. **25**, 237–253 (2001)
2. Gendelman, O.V., Vakakis, A.F., Manevitch, L.I., McCloskey, R.: Energy pumping in nonlinear mechanical oscillators I: Dynamics of the underlying Hamiltonian system. J. Appl. Mech. **68**(1), 34–41 (2001)
3. Vakakis, A.F., Gendelman, O.V.: Energy pumping in nonlinear mechanical oscillators II: resonance capture. J. Appl. Mech. **68**(1), 42–48 (2001)
4. Vakakis, A.F.: Inducing passive nonlinear energy sinks in linear vibrating systems. J. Vib. Acoust. **123**(3), 324–332 (2001)
5. Vakakis, A.F., Manevitch, L.I., Gendelman, O., Bergman, L.: Dynamics of linear discrete systems connected to local essentially nonlinear attachments. J. Sound Vib. **264**, 559–577 (2003)
6. Vakakis, A.F., Gendelman, O., Bergman, L.A., McFarland, D.M., Kerschen, G., Lee, Y.S.: Nonlinear Targeted Energy Transfer in Mechanical and Structural Systems. Springer, Berlin (2009). ISBN 978-1-4020-9125-4. http://www.springer.com/engineering/book/978-1-4020-9125-4
7. Bellet, R., Cochelin, B., Herzog, P., Mattei, P.O.: Experimental study of targeted energy transfer from an acoustic system to a nonlinear membrane absorber. J. Sound Vib. **329**, 2768–2791 (2010)
8. Gatti, G., Kovacic, I., Brennan, M.J.: On the response of a harmonically excited two degree-of-freedom system consisting of a linear and a nonlinear quasi-zero stiffness oscillator. J. Sound Vib. **329**, 1823–1835 (2010)
9. Gatti, G., Brennan, M.J., Kovacic, I.: On the interaction of the responses at the resonance frequencies of a nonlinear two degrees-of-freedom system. Physica D **239**, 591–599 (2010)
10. Gendelman, O.V.: Bifurcations of nonlinear normal modes of linear oscillator with strongly nonlinear damped attachment. Nonlinear Dyn. **37**(2), 115–128 (2004)
11. Shaw, S.W., Pierre, C.: Normal modes for nonlinear vibratory systems. J. Sound Vib. **164**, 85–124 (1993)
12. Vakakis, A.F., Manevitch, L.I., Mikhlin, Yu.V., Pilipchuk, V.N., Zevin, A.A.: Normal Modes and Localization in Nonlinear Systems. Wiley Interscience, New York (1996)
13. Jang, X., McFarland, M., Bergman, L.A., Vakakis, A.F.: Steady state passive nonlinear energy pumping in coupled oscillators: Theoretical and experimental results. Nonlinear Dyn. **33**, 7–102 (2003)
14. Gendelman, O.V., Gourdon, E., Lamarque, C.H.: Quasiperiodic energy pumping in coupled oscillators under periodic forcing. J. Sound Vib. **294**, 651–662 (2006)
15. Gendelman, O.V., Starosvetsky, Y.: Quasiperiodic response regimes of linear oscillator coupled to nonlinear energy sink under periodic forcing. ASME J. Appl. Mech. **74**, 325–331 (2007)
16. Gendeman, O.V., Starosvetsky, Y., Feldman, M.: Attractors of harmonically forced linear oscillator with attached nonlinear energy sink I: Description of response regimes. Nonlinear Dyn. **51**, 31–46 (2008)
17. Starosvetsky, Y., Gendelman, O.V.: Attractors of harmonically forced linear oscillator with attached nonlinear energy sink II: Optimization of a nonlinear vibration absorber. Nonlinear Dyn. **51**, 47–57 (2008)
18. Starosvetsky, Y., Gendelman, O.V.: Strongly modulated response in forced 2DOF oscillatory system with essential mass and potential asymmetry. Phys. D, Nonlinear Phenom. **237**(13), 1719–1733 (2008)
19. Starosvetsky, Y., Gendelman, O.V.: Dynamics of a strongly nonlinear vibration absorber coupled to a harmonically excited two-degree-of-freedom system. J. Sound Vib. **312**, 234–256 (2008)

20. Starosvetsky, Y., Gendelman, O.V.: Interaction of nonlinear energy sink with a two degrees of freedom linear system: Internal resonance. J. Sound Vib. **329**, 1836–1852 (2009)
21. Starosvetsky, Y., Gendelman, O.V.: Vibration absorption in systems with a nonlinear energy sink: nonlinear damping. J. Sound Vib. **324**, 916–939 (2009)
22. Manevitch, L.I.: Complex representation of dynamics of coupled nonlinear oscillators. In: Mathematical Models of Non-Linear Excitations. Transfer, Dynamics, and Control in Condensed Systems and Other Media, pp. 269–300. Kluwer Academic/Plenum, Dordrecht/New York (1999)